## Original Article

# Salinity-Induced Stability Transitions of SiO<sub>2</sub> and Al<sub>2</sub>O<sub>3</sub> Nanoparticles for Enhanced Oil Recovery Applications

Muhammad Hamza<sup>1\*</sup>, Musa Momoh<sup>1</sup>, Faruk Sani<sup>1</sup>, and Lawal Sa'ad<sup>2</sup>

<sup>1</sup>Department of Physics, Usmanu Danfodiyo University, Sokoto, Nigeria. <sup>2</sup>Department of Physics, Federal University, Gusau, Nigeria.

\*Corresponding Author: muhammad.hamza2e@gmail.com;

Received: 03 June 2025 Revised: 10 July 2025 Accepted: 28 July 2025 Published: 13 August 2025

**Abstract** - In order to assess the behavior of  $SiO_2$  and  $Al_2O_3$  nanoparticles for possible use in enhanced oil recovery (EOR), this study examines their dispersion stability under varying salinity (0.1-2.0 M) and concentration (0.01-3.0 wt%). At 0.1 M ionic strength, SiO<sub>2</sub> nanoparticles showed good stability, especially below 1 wt%, where electrostatic repulsion was maintained (zeta potential: -9.52 to -15.02 mV) and sedimentation was mild. Larger hydrodynamic diameters (up to 895.88 nm) and noticeable sedimentation, particularly at higher concentrations, were the result of ionic charge screening, which caused zeta potentials to decrease as salinity rose to 1.0 M and 2.0 M. These patterns supported a gradual destabilization brought on by a decrease in electrostatic repulsion. However, because of their larger size and intrinsic positive surface charge, Al<sub>2</sub>O<sub>3</sub> nanoparticles exhibited different behavior. While increasing concentration at 0.1 M resulted in early aggregation and sedimentation, it improved surface charge (zeta potential: +7.92 to +15.20 mV). Higher ionic strength compressed the electrical double layer at 1.0 and 2.0 M, causing severe aggregation and sedimentation at all concentrations, even though zeta potentials remained high (+12.5 to +21.2 mV). Significantly, this shows that zeta potential alone is not a reliable indicator of stability in high salinity systems. Overall, although both nanoparticles show some dispersion stability at low concentrations ( $\leq 0.1 \text{ wt}\%$ ) and salinity, stability decreases with ionic strength due to van der Waals attraction, double-layer compression, and charge screening. Surface modification or salinity control is needed for performance in high-salinity EOR.

**Keywords -** Aggregation, Alumina nanoparticles, Enhanced oil recovery, Interfacial tension, Silica nanoparticles.

# 1. Introduction

Nanoparticles' unique characteristics, like their large surface area, adjustable surface chemistry, and increased reactivity, have attracted a lot of attention in a variety of sectors. Silicon dioxide (SiO<sub>2</sub>) and aluminum oxide (Al<sub>2</sub>O<sub>3</sub>) nanoparticles, in particular, have gained considerable attention for their ability to modify rock wettability, reduce interfacial tension (IFT), and stabilize emulsions during EOR processes[1]. However, the dispersion stability of these nanoparticles in various environments, particularly in brine with high salinity, is crucial to their efficacy in such applications [2].

The ability of nanoparticles to stay uniformly distributed in a suspension without settling or aggregating over time is known as dispersion stability. In many real-world applications, this stability is essential. Nanoparticles used in Enhanced Oil Recovery (EOR) must maintain their stability under the severe circumstances of subsurface reservoirs. which frequently contain brine with high salinity. Under these circumstances, nanoparticle aggregation or sedimentation can drastically diminish their efficacy and impede their passage through porous media [3].

In many applications, dispersion stability is a critical property of the nanoparticles that determines their effectiveness and performance. For instance, Van der Waals attraction and electrostatic repulsion are two types of interparticle forces that impact the stability of a suspension of nanoparticles in a colloidal system[4]. The Derjaguin-Landau-Verwey-Overbeek (DLVO) theory describes these forces and predicts the conditions under which the particles will stay dispersed or aggregate [3][4]. The high ion concentration presents a distinctive problem for the dispersion stability of nanoparticles in high salinity brine. These ions may also enhance aggregation due to their ability to screen electrostatic repulsion between nanoparticles [2] [4].

This phenomenon is often described by the DLVO (Derjaguin, Landau, Verwey, and Overbeek) theory, which takes into account the van der Waals attraction and the electrostatic repulsion to account for the stability of the colloidal systems[5]. According to the DLVO theory, increased ionic strength is capable of lowering the electrostatic double layer around the nanoparticles, which, in turn, decreases the repulsive forces and therefore adds to aggregation [5], [6].



Aluminum oxide and silicon dioxide nanoparticles are prevalent in the industry due to their chemical stability, mechanical strength, and ease of obtaining functional groups. The silicon dioxide nanoparticles are particularly known for their large surface area, biocompatibility, and the capability of forming stable suspensions in water [7].

On the other hand, aluminum nanoparticles have significant thermal stability, mechanical strength, and greater catalytic activity, enabling their use in catalysis and water purification [8]. In order to maximize the effectiveness of the nanoparticles in these applications, EOR processes like enhanced oil recovery require an understanding of the stability of these nanoparticles in high salinity brine. The nanoparticles modify rock wettability and reduce the interfacial tension [9].

To characterize nanoparticle stability in such environments, zeta potential, UV-Vi's spectroscopy, and Dynamic Light Scattering (DLS) are widely used [10]. Zeta potential measures the potential difference at the slipping plane of a particle and is a direct indicator of electrostatic stability. Larger absolute values typically correlate with better dispersion. DLS provides information about particle size distribution and aggregation over time, while UV-Vi's spectroscopy allows monitoring of sedimentation and absorbance changes, indicating particle stability [10], [11].

In enhanced oil recovery (EOR) processes, high ionic strength results in the shrinking of the electrical double layer, reducing zeta potential and increasing the likelihood of particle aggregation [12]. Research performed with silica (SiO<sub>2</sub>) and alumina (Al<sub>2</sub>O<sub>3</sub>) nanoparticles showed that with increasing ionic strength, the zeta potential of the nanoparticles decreased, which diminished the stability and transport of the nanoparticles within the porous media [12][13].

Rahmadiawan and Shi [14] examined the zeta potential of SiO<sub>2</sub> and Al<sub>2</sub>O<sub>3</sub> nanoparticles in aqueous suspensions and observed that elevated ionic strengths diminished zeta potential and, in turn, stability.

Jiang et al. [15] reported that SiO<sub>2</sub> nanoparticles exhibit good dispersion at lower concentrations but begin to aggregate in synthetic seawater with elevated salinity. Similarly, Said et al.[16] found that Al<sub>2</sub>O<sub>3</sub> nanoparticles exhibit increased aggregation as salt concentration rises.

The use of nanoparticles in enhancing oil recovery (EOR) processes is promising; however, their use in high salinity reservoirs faces problems with stability. SiO<sub>2</sub> and Al<sub>2</sub>O<sub>3</sub> nanoparticles have received some attention, but much of the work is either focused on just one type of nanoparticle or using just one method of characterization. This is particularly important in the context of how these nanoparticles function in actual reservoir conditions. Additionally, the lack of zeta potential, UV-Vis spectroscopy, and DLS cross-nanoparticle

comparisons indicates the need for systematic and holistic studies.

To address this gap, the present study investigates the stability of silicon dioxide and aluminum oxide nanoparticles in high-salinity brine. By employing a combination of zeta potential measurements, UV-Vis spectroscopy, and particle size analysis via DLS, this research aims to better understand how nanoparticle type and brine salinity affect dispersion stability. The findings are intended to inform the selection and formulation of more stable nanofluids for enhanced oil recovery applications.

## 2. Materials and Methods

#### 2.1. Materials

In this research, two available commercial NPs, namely, silicon dioxide NP (SiO<sub>2</sub>, with 99.9% purity, size of 20nm-30nm, specific surface area of 100-500m<sup>2</sup>/g and aluminium oxide NP (Al<sub>2</sub>O<sub>3</sub>, with 99% purity, size of 20–30nm and specific surface area of 50m<sup>2</sup>/g to 150m<sup>2</sup>/g), and Sodium chloride (NaCl) of 181.164g were purchased from Guangdong GuanghuaSci-Tech Co., Ltd, China. Nanoparticle concentrations, (NaCl) saline solution, Dispersion Medium (deionized water).

Apparatus: Ultrasonic bath, Centrifuge, Zeta potential analyzer, UV-Vis spectrophotometer, Dynamic Light Scattering (DLS) equipment, Analytical balance, Vials and beakers, Magnetic stirrer

Table 1. Properties of nanoparticles

Properties	SiO <sub>2</sub>	Al <sub>2</sub> O <sub>3</sub>
Appearance	Dispersion	White powder
Particle size	20nm-30nm	20nm-30nm
Specific Surface	100 5002/	$50m^{2}/g$ -
Area	$100-500 \mathrm{m^2/g}$	150m/g
Purity	99.9%	99%
Density	$0.25 \mathrm{g/cm^3}$	$0.2 - 0.6 \text{g/cm}^3$

## 3.1. Methods

# 3.1.1. Sample Preparation

6.66g of both SiO<sub>2</sub> and Al<sub>2</sub>O<sub>3</sub> nanoparticles were weighed out to prepare suspensions at the desired concentrations of 0.01 wt%, 0.05 wt%, 0.1 wt%, 0.5 wt%, 1.0 wt%, 2.0 wt%, and 3.0 wt%. The nanoparticles were then dispersed in deionized water using an ultrasonic bath for 30 minutes to ensure a uniform suspension.

The brine solutions of different ionic strengths (0.1 M, 1 M, and 2 M) were prepared by dissolving NaCl(181.164g) in deionized water. The prepared nanoparticle suspensions were added to the brine solutions to achieve the desired final concentrations of nanoparticles. A magnetic stirrer was used to mix the solutions thoroughly for at least 30 minutes.

The mixed solutions were then subjected to ultrasonication for another 30 minutes to break any aggregates and ensure a homogeneous dispersion. The mixed solutions were divided into several vials for subsequent analysis.

## 3.1.2. Methodology

The stability testing involved transferring nanoparticlebrine mixtures into glass vials for systematic observation and analysis. Each concentration was tested under different brine conditions, labeled with nanoparticle type, concentration, and ionic strength. Vials were stored under controlled conditions and observed at various time points. Some vials were used for zeta potential, DLS, UV-Vis, and centrifugation tests to quantitatively assess stability.

A zeta potential analyzer was used to measure the zeta potential of nanoparticle suspensions prepared in brine solutions of varying salinities. Higher absolute zeta potential values, whether positive or negative, were interpreted as indicative of better dispersion stability due to stronger electrostatic repulsion between particles. Prior to measurement, all suspensions were sonicated to ensure uniform dispersion and then allowed to equilibrate at room temperature (~25°C).

A portion of each equilibrated sample was then loaded into the zeta potential measurement cell, typically a folded capillary cell or dip cell. The analyzer applied an electric field across the sample, and the electrophoretic mobility of the nanoparticles was measured using laser Doppler velocimetry (LDV), which detects the frequency shift of scattered light caused by particle motion.

The resulting electrophoretic mobility was then automatically converted into zeta potential ( $\zeta$ -potential) using the Henry equation,

$$\int = \frac{3\eta\mu}{2ef(ka)} \tag{1}$$

 $\int$ : zeta potential(mv),  $\mu$ : electrophoretic mobility,  $\eta$ : viscosity of the medium,  $\epsilon$ : Dielectric constant of the medium, F(ka): Henry function.

This accounts for medium viscosity, dielectric constant, and ionic strength. To ensure measurement accuracy and repeatability, each concentration was analyzed in triplicate, and the average zeta potential value was recorded. All measurements were conducted under identical environmental and instrumental conditions to minimize variability and ensure data reliability across all test conditions.

The DLS analyzer was calibrated, and a nanoparticle suspension was transferred to a cuvette. A laser beam was directed, and the intensity of scattered light was analyzed. The hydrodynamic diameter was determined using the Stokes-Einstein equation. The UV-Vis spectrophotometer was calibrated, and a suspension was transferred to a cuvette. Absorption was recorded at specific wavelengths, with a full scan to determine the maximum absorption wavelength for each nanoparticle type.

The samples were centrifuged at 3000 rpm for 30 minutes to accelerate sedimentation. The supernatant was visually compared for clarity, with clear samples indicating poor nanoparticle stability. Sediment volume measurement was noted, and UV-Vis spectroscopy was used to quantify the concentration of dispersed nanoparticles.

The stability of  $SiO_2$  and  $Al_2O_3$  nanoparticles was evaluated under various salinity conditions using zeta potential measurements, particle size distribution (DLS), and UV-Vis spectroscopy. Data was analyzed to observe dispersion behavior trends across concentrations. Results showed changes in surface charge, hydrodynamic diameter, particle size, and aggregation, as well as absorption values and sedimentation trends.

## 4. Results and Discussion

Table 2. Stability of SiO<sub>2</sub> Nanoparticles at 0.1 M Ionic Strength

Conc. (wt.%)	Zeta Potential (mV)	Hydrodynamic Diameter (nm)	Absorbance	Sedimentation Observation
0.01	-9.52	225.10	0.612	Minimal sedimentation
0.05	-10.74	260.85	0.791	Minimal sedimentation
0.1	-11.37	301.65	0.933	Minimal sedimentation
0.5	-12.96	395.80	1.681	Minimal sedimentation
1.0	-13.73	673.14	2.082	Minimal sedimentation
2.0	-14.21	712.55	2.480	Slight aggregation; moderate sedimentation
3.0	-15.02	790.33	2.743	Moderate aggregation; moderate sedimentation

Table 3. Stability of SiO<sub>2</sub> Nanoparticles at 1.0 M Ionic Strength

Conc. (wt.%)	Zeta Potential (mV)	Hydrodynamic Diameter (nm)	Absorbance	Sedimentation Observation
0.01	-5.30	160.30	0.327	Moderate sedimentation
0.05	-6.10	180.12	0.435	Moderate sedimentation
0.1	-6.80	195.60	0.519	Moderate sedimentation
0.5	-7.40	530.22	1.260	Noticeable aggregation; moderate sedimentation
1.0	-8.10	600.07	1.856	Moderate sedimentation
2.0	-8.50	755.33	2.121	Noticeable aggregation; high sedimentation
3.0	-9.00	840.62	2.405	Strong aggregation; high sedimentation

Table 4. Stability of SiO<sub>2</sub> Nanoparticles at 2.0 M Ionic Strength

Conc. (wt.%)	Zeta Potential (mV)	Hydrodynamic Diameter (nm)	Absorbance	Sedimentation Observation
0.01	-4.80	290.25	0.551	Slight aggregation; moderate sedimentation
0.05	-5.30	305.60	0.684	Slight aggregation; moderate sedimentation
0.1	-5.90	315.55	0.976	Slight aggregation; moderate sedimentation
0.5	-6.50	550.75	1.792	Significant aggregation; high sedimentation
1.0	-7.10	611.06	1.890	Significant aggregation; high sedimentation
2.0	-7.60	801.44	2.270	Significant aggregation; very high sedimentation
3.0	-8.00	895.88	2.633	Severe aggregation; very high sedimentation

Table 5. Stability of Al<sub>2</sub>O<sub>3</sub> Nanoparticles at 0.1 M Ionic Strength

Conc. (wt.%)	Zeta Potential (mV)	Hydrodynamic Diameter (nm)	Absorbance	Sedimentation Observation
0.01	+7.92	430.20	1.182	Moderate sedimentation
0.05	+8.72	470.85	1.349	Moderate sedimentation
0.1	+10.80	543.65	1.681	Moderate sedimentation
0.5	+11.67	678.20	1.913	High sedimentation
1.0	+13.35	566.70	1.752	Moderate sedimentation
2.0	+14.60	720.15	2.019	High sedimentation
3.0	+15.20	782.60	2.219	High sedimentation; early aggregation

Table 6. Stability of Al<sub>2</sub>O<sub>3</sub> Nanoparticles at 1.0 M Ionic Strength

Conc. (wt.%)	Zeta Potential (mV)	Hydrodynamic Diameter (nm)	Absorbance	Sedimentation Observation
0.01	+12.5	525.90	1.654	Significant sedimentation
0.05	+14.2	590.10	1.842	High sedimentation
0.1	+15.8	651.35	2.014	Significant sedimentation
0.5	+17.6	728.55	2.135	Strong sedimentation
1.0	+19.3	776.30	2.398	High sedimentation
2.0	+20.5	845.10	2.601	Very high sedimentation
3.0	+21.2	910.20	2.802	Severe aggregation; very high sedimentation

Table 7. Stability of Al<sub>2</sub>O<sub>3</sub> Nanoparticles at 2.0 M Ionic Strength

Conc. (wt.%)	Zeta Potential (mV)	Hydrodynamic Diameter (nm)	Absorbance	Sedimentation Observation
0.01	+15.20	565.60	1.802	Aggregation; moderate sedimentation
0.05	+16.80	595.40	1.865	Moderate aggregation; high sedimentation
0.1	+17.50	597.90	1.846	Aggregation; moderate sedimentation
0.5	+18.90	765.60	2.213	Significant aggregation; high sedimentation
1.0	+19.80	810.45	2.503	Strong aggregation; very high sedimentation
2.0	+20.10	890.85	2.690	Strong aggregation; very high sedimentation
3.0	+20.60	960.45	2.973	Severe aggregation; extreme sedimentation

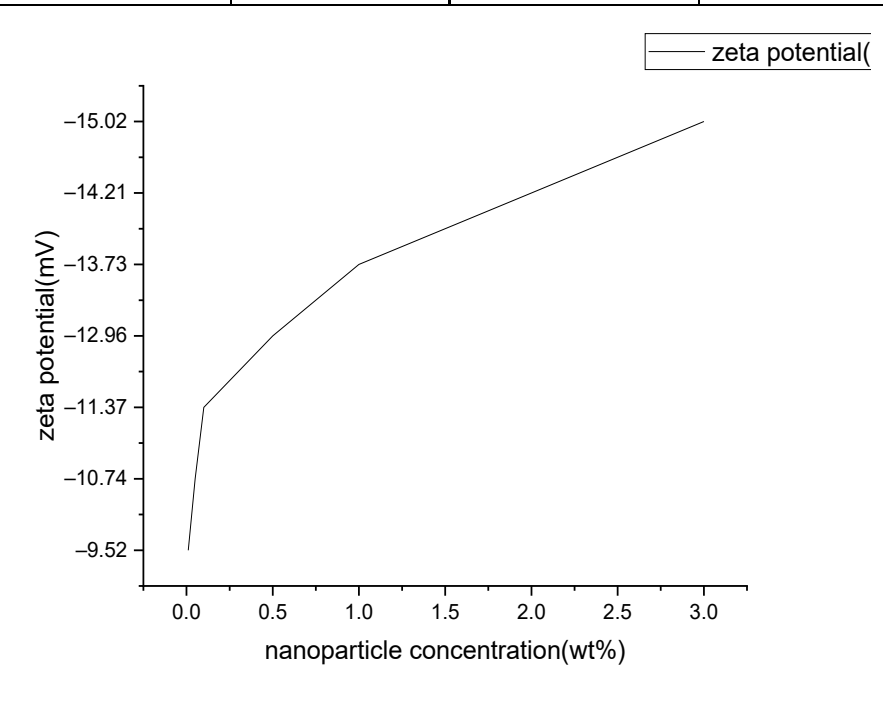


Fig. 1 Stability of SiO<sub>2</sub> Nanoparticles at 0.1 M Ionic Strength

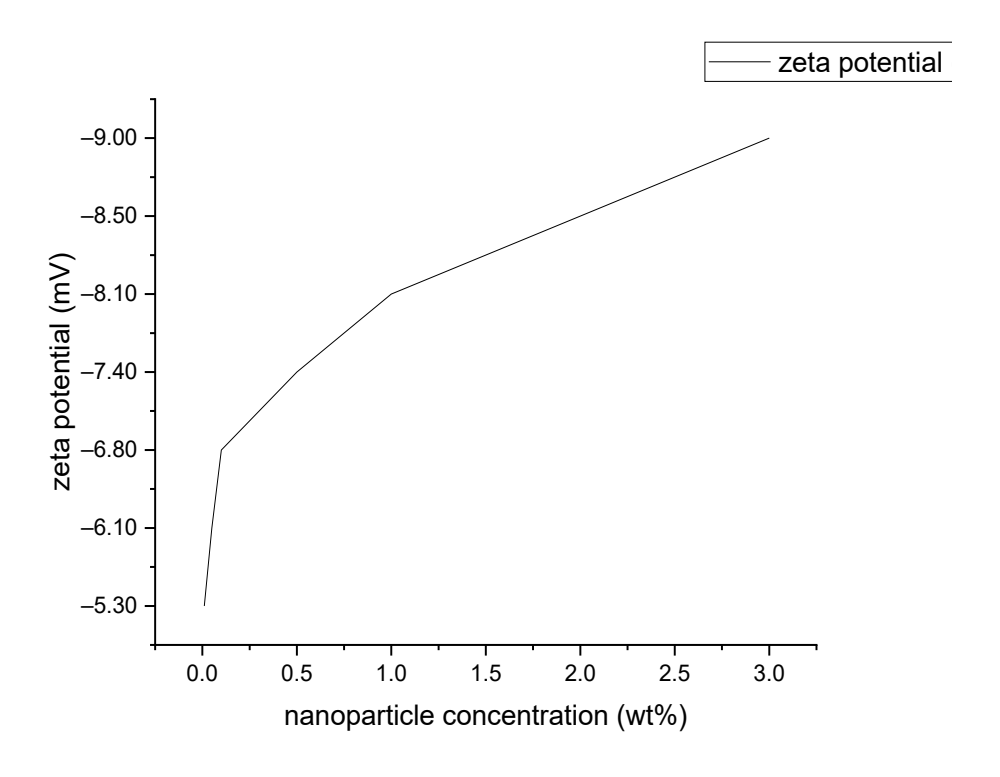


Fig. 2 Stability of SiO<sub>2</sub> Nanoparticles at 1.0 M Ionic Strength

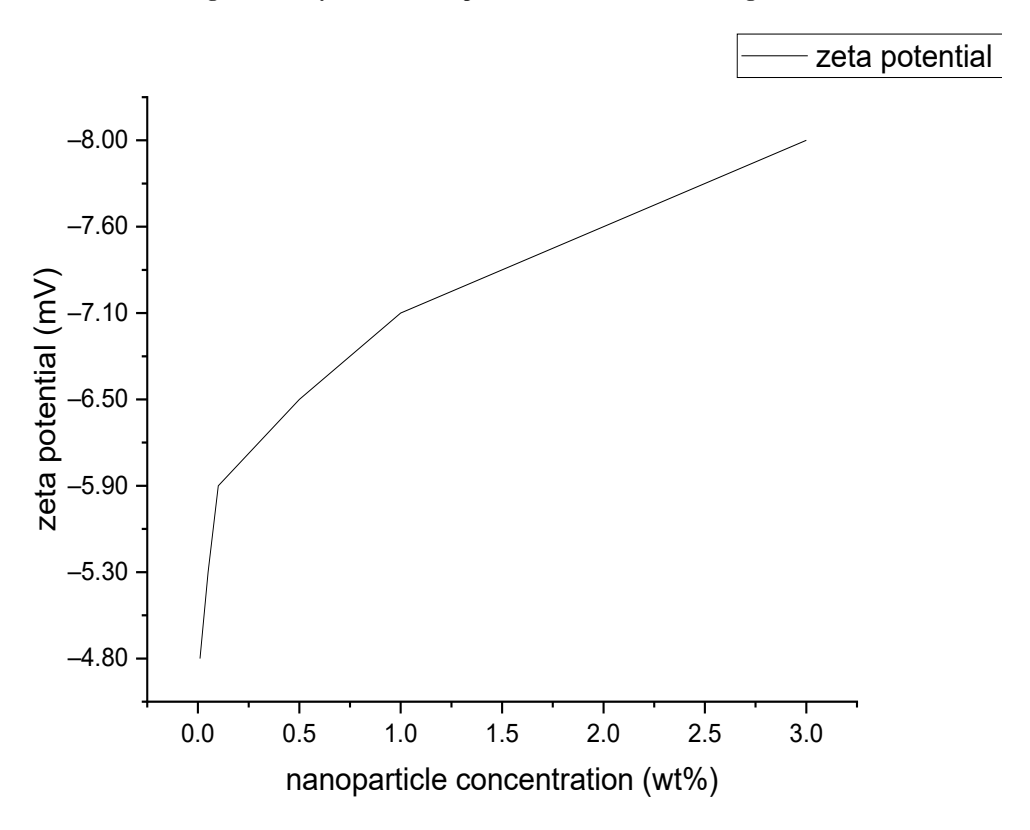


Fig. 3 Stability of SiO<sub>2</sub> Nanoparticles at 2.0 M Ionic Strength

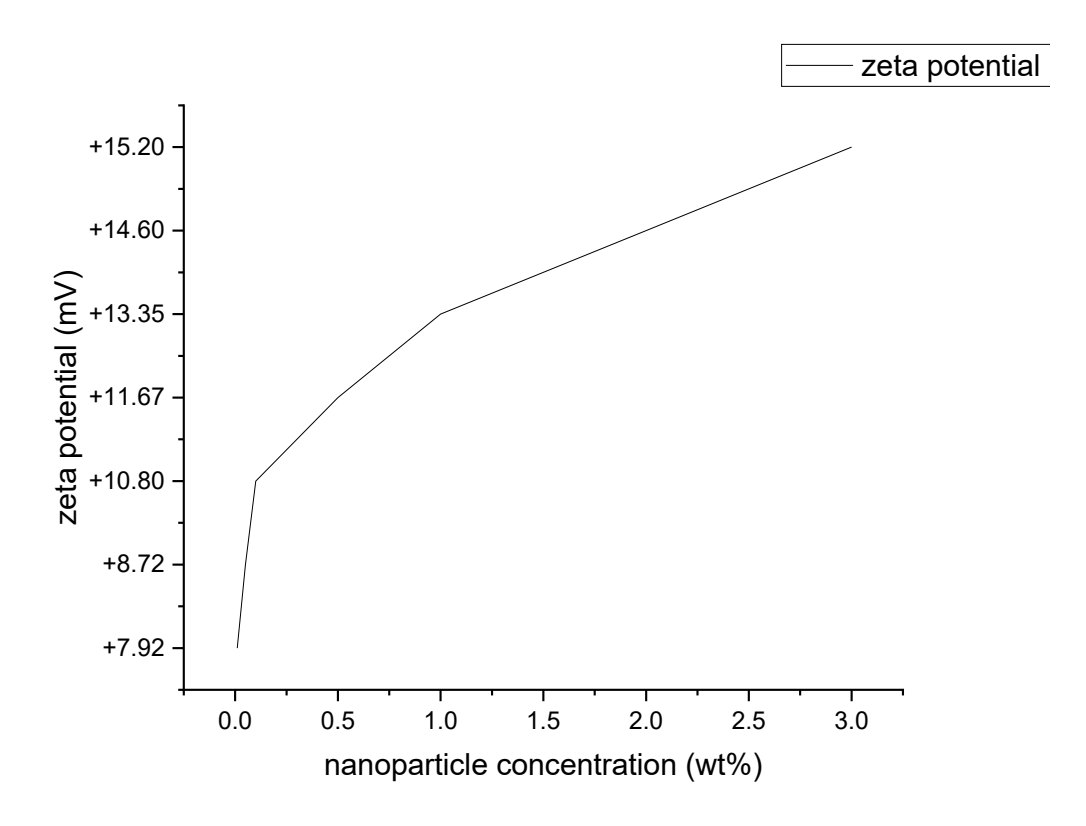


Fig. 4 Stability of Al<sub>2</sub>O<sub>3</sub> Nanoparticles at 0.1 M Ionic Strength

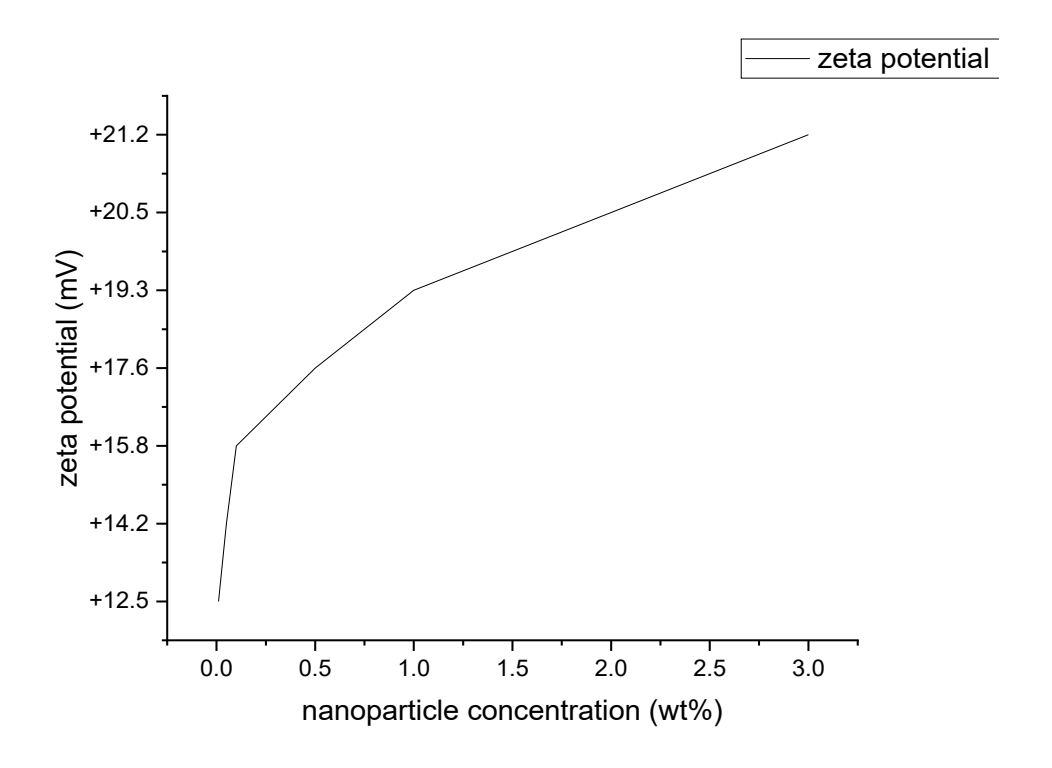


Fig. 5 Stability of Al<sub>2</sub>O<sub>3</sub> Nanoparticles at 1.0 M Ionic Strength

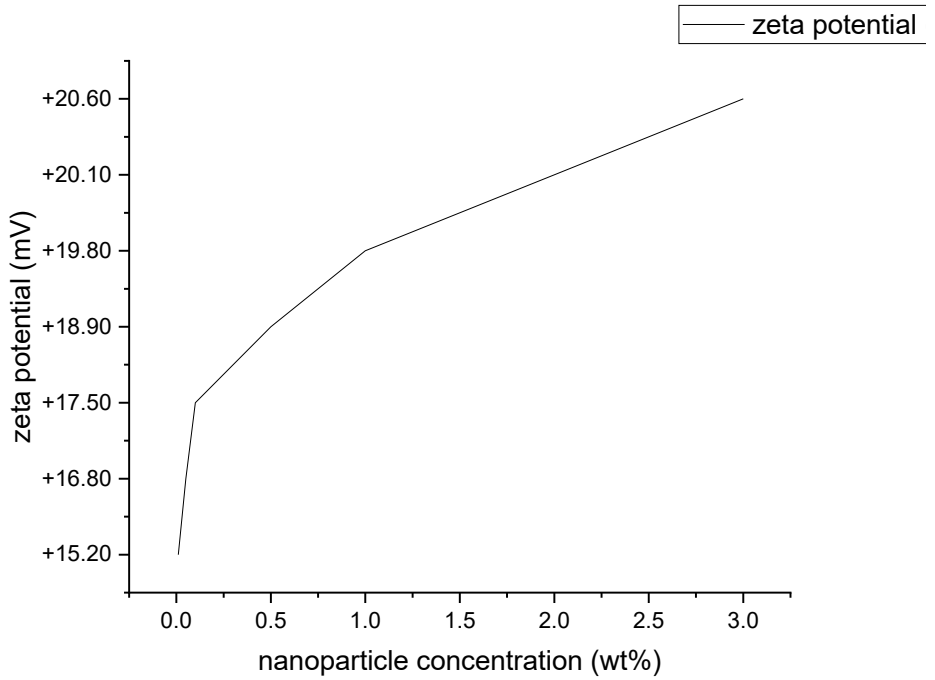


Fig. 6 Stability of Al<sub>2</sub>O<sub>3</sub> Nanoparticles at 2.0 M Ionic Strength

#### 4.1. Discussion

The stability behavior of SiO<sub>2</sub> nanoparticles across different salinity levels reveals a clear trend influenced by both ionic strength and particle concentration. Relatively good stability was observed at 0.1 M ionic strength. A slight increase in electrostatic repulsion was indicated by zeta potential values, which ranged from -9.52 mV to -15.02 mV as concentration increased from 0.01 to 3.0 wt%, as shown in Table 2 and further illustrated in Figure 1. Additionally, the hydrodynamic diameter increased steadily from 225.10 nm to 790.33 nm, indicating some clustering at higher concentrations, as also detailed in Table 2. Despite this, the absorbance remained high and sedimentation was mild to moderate, suggesting that the dispersions were generally stable under low-salinity conditions, particularly at concentrations below 1 wt%.

The zeta potential values decreased from -5.30 mV to -9.00 mV as the salinity rose to 1.0 M, indicating a notable decrease in electrostatic repulsion caused by charge screening from the ions in solution, as shown in Table 3 and further illustrated in Figure 2. Particle size increased and aggregation became more noticeable; hydrodynamic diameters ranged from 160.30 nm at 0.01 wt% to 840.62 nm at 3.0 wt%, as detailed in Table 3. Although absorbance values increased with concentration, they were accompanied by moderate to high sedimentation and visible aggregation—especially above 0.5 wt%—which indicated the onset of instability.

The instability increased at 2.0 M, the highest salinity level. Over the concentration range, the particles' hydrodynamic size rapidly increased from 290.25 nm to

895.88 nm, and their zeta potentials decreased even more (from -4.80 mV to -8.00 mV) as shown in Table 4 and Figure 3. Even at low concentrations, there was significant to severe sedimentation because the decreased surface charge was no longer able to stop aggregation. At 3.0 wt%, absorbance peaked at about 2.633, but this was accompanied by extremely high sedimentation, indicating that a significant portion of the mass of the nanoparticles was settling out of suspension, as shown in Table 4.

These findings show that SiO₂ nanoparticle dispersions are weakly stable at low salinity and grow more unstable as ionic strengths increase due to decreased electrostatic repulsion. Lower concentrations (≤0.1 wt%) provide greater stability at all salinities, but higher concentrations cause sedimentation and aggregation, especially in 1.0 M and higher brines. This emphasizes how enhanced oil recovery applications require surface modification or salinity control to preserve nanoparticle stability and efficacy in high-salinity reservoir environments.

In the case of aluminium oxide, Al<sub>2</sub>O<sub>3</sub> nanoparticles show unique stability under increasing salinity and concentration conditions due to larger particle size and positive surface charge, influenced by particle-particle interactions, hydration shell compression, and ionic bridging.

At 0.1 M ionic strength, Al<sub>2</sub>O<sub>3</sub> nanoparticles exhibited relatively positive zeta potentials, increasing from +7.92 mV to +15.20 mV with rising concentration, as shown in Table 5 and Figure 4. This suggests improved surface charge due to protonation. Despite this, moderate to high sedimentation

occurred, especially at higher concentrations. Hydrodynamic diameters increased from 430.20 nm to 782.60 nm, indicating gradual aggregation. Absorbance rose steadily, peaking at 2.219 at 3.0 wt%, mainly due to light scattering by large aggregates. Aggregation signs appeared as early as 3.0 wt%. Stability was only conditional, with dispersions tending toward sedimentation beyond 0.5 wt%. Overall, the dispersions were not fully stable even in low-salinity conditions.

At 1.0 M ionic strength, Al<sub>2</sub>O<sub>3</sub> nanoparticles showed an increase in zeta potential from +12.5 to +21.2 mV, most likely due to enhanced ion adsorption, as shown in Table 6 and Figure 5. However, this increase did not lead to improved stability. The compressed electrical double layer promoted van der Waals attraction and aggregation. Significant growth in hydrodynamic diameter (from 525.90 nm to 910.20 nm) and absorbance (1.654 to 2.802) was observed, as shown in Table 6. These increases were accompanied by severe sedimentation and visible aggregation. Most particles were no longer in stable suspension. This demonstrates that zeta potential alone is not a reliable predictor of stability in high-salinity systems. Al<sub>2</sub>O<sub>3</sub> dispersions remained unstable despite a high surface charge.

At an Ionic Strength of 2.0, across all concentrations, Al<sub>2</sub>O<sub>3</sub> nanoparticles showed obvious signs of instability under this high salinity condition. Even at 0.01 wt%, the dispersions suffered from aggregation and heavy sedimentation, despite the constant high zeta potential values (+15.20 to +20.60 mV), as shown in Table 7 and Figure 6.

This emphasizes once more that under such ionic strength, electrostatic stabilization is insufficient. Sedimentation observations also ranged from moderate to extreme, with terms like severe aggregation and very high sedimentation dominating the description, especially beyond 0.5 wt.%. The hydrodynamic diameter values increased significantly (from 565.60 nm to 960.45 nm), and absorbance

reached a maximum of 2.973 at 3.0 wt.%, the highest across all conditions tested, as shown in Table 7.

### 5. Conclusion

This study thoroughly assessed the dispersion stability of SiO<sub>2</sub> and Al<sub>2</sub>O<sub>3</sub> nanoparticles under a range of salinity conditions and particle concentrations to ascertain their suitability for enhanced oil recovery (EOR) applications. SiO<sub>2</sub> exhibited the highest dispersion stability at low salinity (0.1 M), especially at concentrations  $\leq$ 0.1 weight percent, where mild sedimentation and relatively negative zeta potentials indicated adequate electrostatic stabilization. As salinity increased to 1.0 M and 2.0 M, zeta potential values decreased and particle aggregation intensified due to ion-induced charge screening, resulting in significant sedimentation and instability, particularly at concentrations  $\geq$ 0.5 wt%.

Al<sub>2</sub>O<sub>3</sub> nanoparticles, on the other hand, demonstrated consistently high positive zeta potentials across all salinity levels, suggesting a high surface charge. This was not, however, the same as dispersion stability. Higher salinities (≥1.0 M) promoted aggregation and sedimentation even at low concentrations due to the compression of the electrical double layer and increased van der Waals forces. The increasing hydrodynamic diameters and absorbance values were primarily due to the formation of large aggregates rather than stable colloidal systems, despite the fact that they demonstrated the presence of particles in suspension.

The limitations of electrostatic stabilization alone in highsalinity conditions were highlighted by the overall decrease in stability observed in both types of nanoparticles as ionic strength increased.

The results suggest that if nanoparticles remain effective in high-salinity EOR applications, other strategies such as surface functionalization, polymer coating, or salinity control must be considered to minimize aggregation and maintain dispersion stability.

## References

- [1] Anirbid Sircar et al., "Applications of Nanoparticles in Enhanced Oil Recovery," *Petroleum Research*, vol. 7, no. 1, pp. 77-90, 2022. [CrossRef] [Google Scholar] [Publisher Link]
- [2] Aly A. Hamouda, and Rockey Abhishek, "Effect of Salinity on Silica Nanoparticle Adsorption Kinetics and Mechanisms for Fluid/Rock Interaction with Calcite," *Nanomaterials*, vol. 9, no. 2, pp. 1-15, 2019. [CrossRef] [Google Scholar] [Publisher Link]
- [3] Anthony Hutin et al., "Stability of Silica Nanofluids at High Salinity and High Temperature," *Powders*, vol. 2, no. 1, pp. 1-20, 2022. [CrossRef] [Google Scholar] [Publisher Link]
- [4] Elmira Dalabayeva, Peyman Pourafshary, and Rizwan Muneer, "DLVO-Based Prediction of Critical pH for Fines Migration in Sandstone Reservoirs," *Petroleum Research*, pp. 1-12, 2025. [CrossRef] [Google Scholar] [Publisher Link]
- [5] Víctor Agmo Hernández, "An Overview of Surface Forces and the DLVO Theory," *ChemTexts*, vol. 9, no. 4, pp. 1-16, 2023. [CrossRef] [Google Scholar] [Publisher Link]
- [6] Namsoon Eom, Drew F. Parsons, and Vincent S. J. Craig, "Roughness in Surface Force Measurements: Extension of DLVO Theory to Describe the Forces between Hafnia Surfaces," *Journal of Physical Chemistry B*, vol. 121, no. 26, pp. 6442-6453, 2017. [CrossRef] [Google Scholar] [Publisher Link]

- [7] Osamah Alomair et al., "Evaluation of the Coupled Impact of Silicon Oxide Nanoparticles and Low-Salinity Water on the Wettability Alteration of Berea Sandstones," *Petroleum Exploration and Development*, vol. 50, no. 4, pp. 934-943, 2023. [CrossRef] [Google Scholar] [Publisher Link]
- [8] Omid Tavakkoli et al., "SDS-Aluminum Oxide Nanofluid for Enhanced Oil Recovery: IFT, Adsorption, and Oil Displacement Efficiency," *ACS Omega*, vol. 7, no. 16, pp. 14022-14030, 2022. [CrossRef] [Google Scholar] [Publisher Link]
- [9] Talha Majeed et al., "A Review on Foam Stabilizers for Enhanced Oil Recovery," *American Chemical Society*, vol. 35, no. 7, pp. 5594-5612, 2021. [CrossRef] [Google Scholar] [Publisher Link]
- [10] Paulo Siani et al., "Modeling Zeta Potential for Nanoparticles in Solution: Water Flexibility Matters," *Journal of Physical Chemistry C*, vol. 127, no. 19, pp. 9236-9247, 2023. [CrossRef] [Google Scholar] [Publisher Link]
- [11] Zeta Potential-Introduction 30min Malvern, 2015. [Online]. Available: https://www.research.colostate.edu/wp-content/uploads/2018/11/ZetaPotential-Introduction-in-30min-Malvern.pdf
- [12] Jianxiang Huang, Damiano Buratto, and Ruhong Zhou, "Probing the Electrostatic Aggregation of Nanoparticles with Oppositely Charged Molecular Ions," *Aggregate*, vol. 4, no. 4, pp. 1-10, 2023. [CrossRef] [Google Scholar] [Publisher Link]
- [13] Ali Mohammad Makbul Tamboli, and Julekha Munaf Tade, "Zeta Potential: A Comprehensive Review," *International Research Journal of Pharmacy and Medical Sciences*, vol. 8, no. 2, pp. 115-124, 2025. [Google Scholar] [Publisher Link]
- [14] Dieter Rahmadiawan, and Shih-Chen Shi, "Enhanced Stability, Superior Anti-Corrosive, and Tribological Performance of Al2O3 Water-based Nanofluid Lubricants with Tannic Acid and Carboxymethyl Cellulose over SDBS as Surfactant," *Scientific Reports*, vol. 14, no. 1, pp. 1-13, 2024. [CrossRef] [Google Scholar] [Publisher Link]
- [15] Pavlo Pinchuk, and Ke Jiang, "Size-Dependent Hamaker Constants for Silver and Gold Nanoparticles," *Physical Chemistry of Interfaces and Nanomaterials XIV*, vol. 9549, 2015. [CrossRef] [Google Scholar] [Publisher Link]
- [16] Zafar Said et al., "Recent Advances on the Fundamental Physical Phenomena Behind Stability, Dynamic Motion, Thermophysical Properties, Heat Transport, Applications, and Challenges of Nanofluids," *Physics Reports*, vol. 946, pp. 1-94, 2022. [CrossRef] [Google Scholar] [Publisher Link]